HiSST: 4th International Conference on
High-Speed Vehicle Science & Technology

22–26 September 2025, Tours, France

Validation of the Fokker-Planck chemistry implementation with the RFZ-ST2 upper stage

Moritz Ertl[1], *Leo Basov*[2,3]

Abstract

This work verifies a recently introduced approach to model chemical reactions as implemented in our kinetic Fokker-Planck (FP) code for an industrial scale space transport problem. The FP method is used as it is able to simulate flows in the rarefied regime above the continuum limit, as found at high altitudes. The FP method provides this physical modelling advantage of a particle method with the computational efficiency needed for the simulations of industrial scale applications. We compare FP simulations of the generic RFZ-ST2 upper stage to computational fluid dynamics (CFD) Navier-Stokes simulations with the DLR TAU code. An artificial flight Mach number of $Ma = 15$ is set to facilitate chemical reactions. We limit ourselves to dissociation and exchange reactions. We compare the flow fields and the surface distributions to validate the implementation. This is done as a step towards the simulation of re-usable launch vehicles at high altitudes in re-entry and re-entry burn situations.

Keywords: *Fokker-Planck, particle method, SPARTA, air chemistry, dissociation, re-usable launch vehicle, upper stage, RFZ model, CFD, TAU, comparison*

1. Introduction

A persisting trend in space transportation is reusable systems. Reusable first stages are becoming an established technology. As the new space companies publish only sparely on their findings, the aerodynamics and aerothermodynamics of reusable systems have been extensively studied by DLR, both numerically [1, 2] and experimentally [3, 4]. An overview of the numerical studies can be found in [5]. However, there is a lack of research on one possible trajectory part, the re-entry burn for a return to launch site of the booster. Furthermore, the development of new reusable upper stages has now started, but so far without any successful commercial operations since the retirement of the Space Shuttle. Both the re-entry burn for the booster and the re-usable upper stages provide new challenges for the numerical investigation of the aerodynamics and aerothermodynamics. The relevant trajectory points are all situated at high altitudes which due to low gas densities, are situated above the continuum limit. Classical computational fluid dynamics (CFD) codes solving the Navier-Stokes equations will not be able to accurately simulate these problems.

To address this challenge and obtain the capability for simulating flight conditions in the rarefied gas regime, we are developing a kinetic Fokker-Planck (FP) method [6] to complement our existing and well established CFD code TAU [7]. The FP method solves the Boltzmann equation and has the additional benefit of being computationally effective for low Knudsen numbers when compared to the Direct Simulation Monte Carlo method (DSMC). The FP method is developed in the framework of the open source particle code SPARTA. The implementation includes modeling for polyatomic gases [8] and has been tested for large scale applications both with a single species [9] and on a nitrogen oxygen mixture [10]. The simulation of a re-entry burn requires additional modeling for chemical reactions when interacting with the plume. Recently a novel approach to model chemical reactions in the FP framework was introduced [11]. Dissociation and exchange reactions have been implemented into the FP code and verified

---

[1] *DLR - Deutsches Zentrum für Luft- und Raumfahrt, AS-RFZ, Göttingen, moritz.ertl@dlr.de*
[2] *DLR - Deutsches Zentrum für Luft- und Raumfahrt, AS-RFZ, Göttingen, leo.basov@dlr.de*
[3] *RWTH Aachen, Applied and Computational Mathematics*

for academic cases. The goal of this work is to test the implementation on a real scale space transport system. For this purpose we are using the RFZ-ST2 upper stage [12] of the open source RFZ model for a generic reusable launcher [13]. We simulate the RFZ-ST2 upper stage in unpowered forward flight at an altitude of $h = 75\,\text{km}$ and prescribe an artificial Mach number of $Ma = 15$ to facilitate chemical reactions. We compare the results to TAU CFD simulations.

This work is a step towards simulating a re-entry burn at high altitude with the Fokker-Planck method. In parallel work is being done on modeling the rocket plume with FP, which is also presented in this conference in [14].

2. Numerical Methods & Parameters

For the CFD simulations we use the DLR TAU code [15] with spacecraft extensions [7], to which we will be refereing as TAU. The TAU code is a second order finite volume solver for sets of conservation equations, in our case the compressible Euler-equations on hybrid structured-unstructured meshes. We simulate with second order spatial accuracy by using the AUSMDV upwinding scheme with a carbuncle fix [16] combined with least squares gradient reconstruction and second order temporal accuracy with a 3-stage explicit Runge-Kutta scheme. We use TAUs two temperature model to account for vibration energy. The relaxation is modeled after Landau-Teller [17] and the relaxation time is obtained according to Millikan and White [18].

For the Fokker-Planck particle simulations we use our in-house implementation in the open-source DSMC code SPARTA [19], to which we will be refering as FP. The FP method numerically solves the Boltzmann equation:

$$\frac{\mathrm{D}f}{\mathrm{D}t} = S_{\text{Boltz}}, \tag{1}$$

where f is the scalar velocity distribution function, t is time, and S_{Boltz} is the Boltzmann collision integral. We approximate the collision operator S_{Boltz} by a Fokker-Planck collision operator S_{FP}:

$$S_{\text{Boltz}} \approx S_{\text{FP}} = -\frac{\partial}{\partial V_i}(A_i f) + \frac{\partial^2}{\partial V_j \partial V_j}\left(\frac{D^2}{2} f\right) \tag{2}$$

where V is the molecule velocity with indices given in the Einstein notation. Eq. (2) can be reformulated as stochastic differential equation which in turn can be solved using a particle method similar to the DSMC approach. The collision step is then replaced by a velocity update of the particles which does not rely on the building of collision pairs making the computational cost of the FP method become independent of the Kn number. The drift coefficient A_i and the diffusion coefficient D of Eq. (2) are model parameters chosen in such a way that production terms calculated using the Boltzmann collision operator are reproduced by the production terms using the FP collision operator [20] with the extension for diatomic gas mixtures based on the master equation ansatz [21]. Gas mixtures are modelled using the approach introduced by Hepp et al. [22, 23]. For the simulations presented in this paper we use the FP cubic model [24]. The chemistry is modelled by a novel approach recently introduced by Basov et al. [11].

Both methods use the temperature dependent modified Arrhenius equation for finite rate chemistry modelling:

$$k_f(T) = A \cdot T^B \exp\left(\frac{E_a}{kT}\right), \tag{3}$$

with the model parameters A, B, and E_a, the Boltzmann constant k and temperature T. TAU uses a slightly different formulation, substituting $c = \frac{E_a}{k}$ and an A which differs by the Avogadro constant N_A as TAU requires reaction rates per cell volume in $\left[\frac{1}{\text{s}}\left(\frac{\text{mol}}{\text{m}^3}\right)^{-\alpha_r}\right]$ and FP uses reactions rates per molecule in $\left[\frac{1}{\text{s}}\right]$.

As this work is a first verification step approaching complex geometries, we limit ourselves to a single dissociation reaction of oxygen:

$$\mathrm{O_2 + O \longrightarrow 3\,O}. \tag{4}$$

The Arrhenius coefficients for the reaction are given in table 1.

Table 1. Arrhenius constants for $O_2 + O \longrightarrow 3\,O$

A	B	C
1.660×10^{-8}	-1.5	8.197×10^{-19}

In previous works we already investigated the influence of the relaxation modelling onto the comparability of the two methods [9, 10]. To match current implementations of mixtures we use averaged Millikan-White parameters for both molecules in TAU. The parameters used for both for O and O_2 are provided in table 2 and the variable hard sphere model parameters for FP are in table 3.

Table 2. CFD Millikan-White Parameters

a	b
92.85	0.0445

Table 3. FP Parameters

Species	d_{ref} / m	T_{ref} / K	ω	Z_{rot}^{∞}	T^* / K	C_1 / K	C_2 / K$^{1/3}$
O_2	3.96×10^{-10}	273.15	0.77	16.5	113.5	19.0	137.0
O	3.0×10^{-10}	273.15	0.80	0.0	0.0	0.0	0.0

3. 0D Reactor

We use a 0D chemical reactor setup to compare the temporal evolution of the reactions with both methods. The reactor is set up as an isochoric cube of edge length $a = 1 \times 10^{-4}$ m with a density $\rho = 4.778 \times 10^{-3}$ kg m^{-3} and a temperature $T = 1000$ K for both methods. The reactor is filled with O_2 with a mass fraction $w_{O_2} = 0.899$ and O with a mass fraction $w_O = 0.111$ for a resulting pressure $p = 13.8 \times 10^3$ Pa. The reaction is limited to the single dissociation reaction from equation 4 running with the Arrhenius constant provided in table 1. The reaction is run with a time step of $dt = 1 \times 10^{-9}$ s for 2×10^4 iterations until $t_{\text{end}} = 2 \times 10^{-5}$ s.

The temporal development of the temperatures and the mass fractions for O_2 and O is compared. The initial comparison showed significant differences in the development of the mass fractions, while the temperatures exhibited a rather good comparison. Due to the reaction rate only depending on the temperature, a further investigation of the modelling was done and it was found that TAU uses the Park [25] approach for the calculating the reaction temperature T_r used in the Arrhenius equation

$$T_r = T^s \, T_{\text{vib}}^{1-s}, \tag{5}$$

where T is the translation temperature, T_{vib} is the vibration temperature and s is the Park exponent which default is $s = 0.7$. To better match the results to the FP modelling, which uses the translation temperature as reaction temperature $T_r = T$, the Park exponent will be set to $s = 1.0$ for the rest of this work. While this influences the results, the Park exponent was not identified as the major cause of the differences.

The significant differences where due to the thermodynamic modelling of the internal energies. TAU provides two ways of modelling, one based on the partition function providing an equation of state, the other is using temperature dependent tabulated values for the enthalpy $H - H(0)$ and the specific heat capacity c_p. For the tabulated values we use the data provided in the ESA report STR246 by Capitelli [26]. The TAU results for the reactor were verified versus the open source chemical kinetics tool Cantera [27] using the tabulated values and one temperature modelling, which will be used for all simulations. The FP internal energies are directly modeled using a continues harmonic oscillator for rotatioanl and discrete harmonic oscillator for vibrational degrees of freedom. Additionally, a per reaction energy change models exothermic and endothermic reactions. In order to harmonise the simulation methods, the heat release of a reaction for the FP simulations was adjusted to match the TAU values, using $\Delta H_{\mathrm{form},O_2} = -6.65 \times 10^{-16}$ J.

This resolved the major discrepancies between the two methods. The results with the above described modifications are shown in figure 1. The figure displays temperature on the left axis and mass fractions for O_2 and O on the right axis over time for both methods. The translation temperature is in very good agreement and also the vibration temperatures have only very small differences, which are assume to be due to slight discrepancies in the relaxation modelling. The development of the mass fractions for both O_2 and O are also in very good agreement. The 0D reactor simulation confirms, that the modeling for both TAU and FP is congruent and that the model parameters are well chosen.

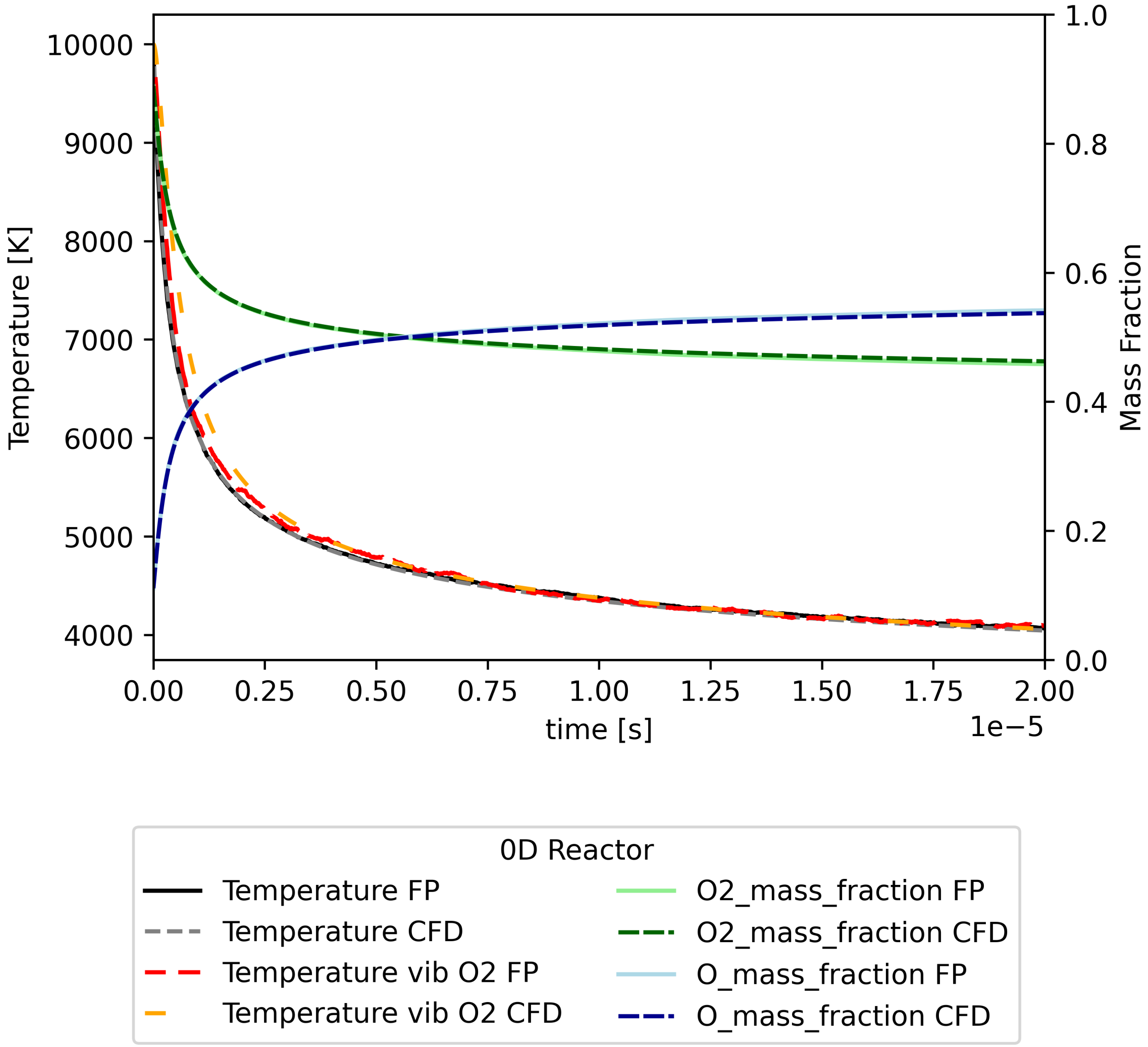

Fig 1. 0D reactor temporal development of temperature and mass fractions.

4. 2D Cylinder

We use a simple case of a 2D cylinder to check the general behaviour of the reaction modelling in a flow. For simplicity we keep O_2 dissociation (equation 4) as the single reaction and use a mixture of O_2

and O as fluid. The cylinder has a diameter of $d_{\text{cyl}} = 0.3\,\text{m}$ with an isothermal wall and the free stream and boundary conditions are provided in table 4 are applied.

Table 4. 2D cylinder case conditions.

Ma_∞	T_∞ / K	ρ_∞ / $\text{kg}\,\text{m}^{-3}$	w_{O_2}	w_{O}	v_∞ / $\text{m}\,\text{s}^{-1}$	T_{W}/K
15	300.0	2.325×10^{-4}	0.899	0.111	5277.6	300.0

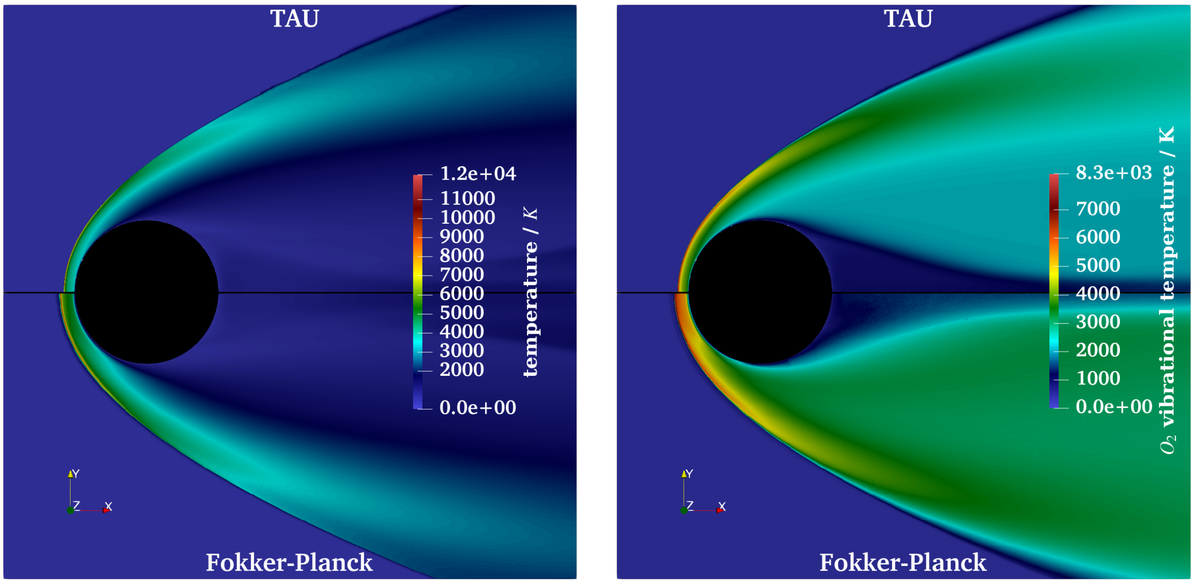

(a) Temperature distribution.

(b) Vibration temperature distribution.

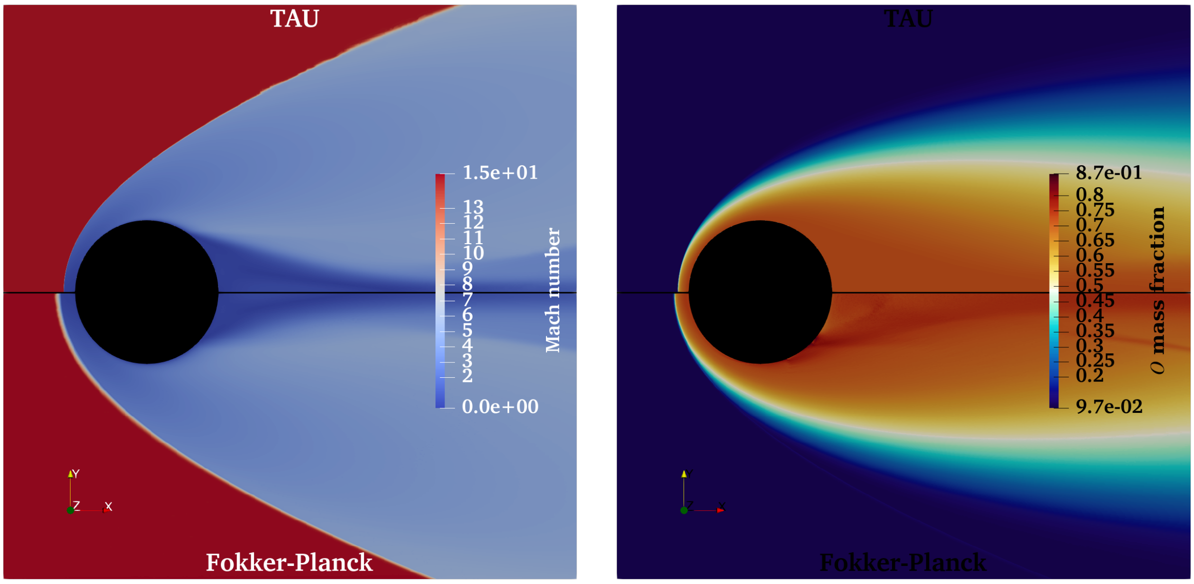

(c) Mach number distribution.

(d) O mass fraction distribution.

Fig 2. Visualisations for the 2D cylinder flow case with $\text{O}_2 + \text{O} \longrightarrow 3\,\text{O}$ dissociation reaction.

The flow field for the most relevant variables temperature T, O_2 vibration temperature $T_{\text{vib},\text{O}_2}$, Mach number Ma and O mass fraction is visualised in figure 2. The general comparison of the flow field displays a good comparison between the two methods. The shape and position of the shocks, as well as the structures in the wake compare well. In all four visualisations we can observe a slight difference in shock stand off distance. This inaccuracy is a known effect of species mixtures in the current FP implementation [10]. It is related to the relaxation in mixtures and will be addressed in the near future. The difference in shock stand off distance is also present in simulations of the cylinder without chemical reactions and is, therefore, not assumed to be a problem of the chemical modelling.

The effect of the chemical reaction can be best observed in figure 2d in the O mass fraction. A large increase in O from $w_{\mathrm{O}} \approx 0.11$ in the free stream to up to $w_{\mathrm{O}} \approx 0.87$ in the regions behind the shock is shown. The dissociation reaction producing the O is driven by the high temperatures behind the shock. The inverse behaviour can be observed for the O_2 mass fractions, which are not shown here. As a result the temperatures in front of cylinder are smaller compared to a non reacting case as seen in figure 2a. While temperature, Mach number and mass fractions compare very well, the comparison of the vibration temperature exhibits more differences. This is in accordance with the above describe issues with the relaxation of mixtures.

A quantitative comparison of the relevant variables is displayed in figure 3 as a plot over the x-center line into the stagnation point. The plot confirms the observations from the flow field. The major difference is in the position of the shock. The translation and vibration temperature peaks at similar values and has a similar, though shifted, shape. The same applies to the mass fractions. The cylinder case shows the validity of our modelling and parameter choice, while highlighting areas of necessary improvement.

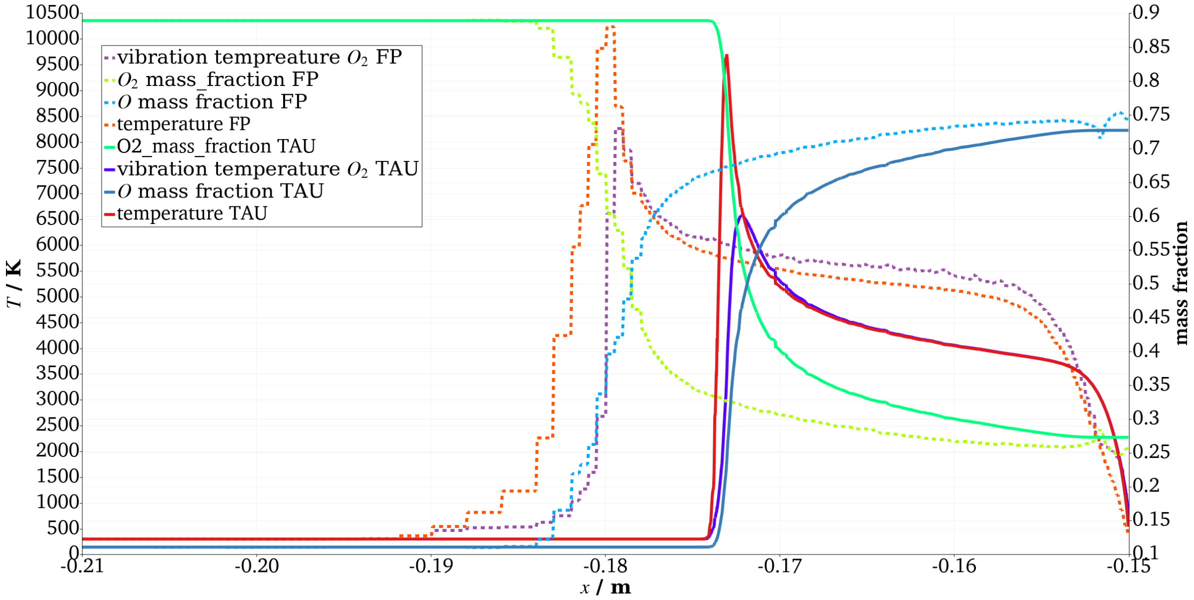

Fig 3. 2D cylinder flow case with $O_2 + O \longrightarrow 3\,O$ dissociation reaction. Stagnation line plot.

5. RFZ upper stage

For the verification for a real scale space transport system, we use the RFZ upper stage geometry RFZ-ST2. We exploit the rotational symmetry to use a 2D setup for both methods. We use the atmospheric conditions for the $h = 75$ km trajectory point, but with an artificially increased Mach number of $Ma = 15$, to facilitate chemical reactions. For simplicity we keep O_2 dissociation (equation 4) as the single reaction and use a mixture of O_2 and O as fluid. The RFZ-ST2 upper stage has a length of $L_{\mathrm{RFZ-ST2}} = 28$ m and has a diameter of $D_{\mathrm{RFZ-ST2}} = 2.6$ m. For boundary conditions we use an isothermal wall with a laminar sublayer. For the free stream the boundary conditions, which are provided in table 5 are applied.

The results of the simulation are shown as visualisations of the flow field in figures 4 and 5. The

Table 5. RFZ-ST2 simulation conditions.

Ma_∞	T_∞ / K	ρ_∞ / kg m^{-3}	w_{O_2}	w_O	v_∞ / m s^{-1}	T_W/K
15	208.34	4.03×10^{-5}	0.899	0.111	4393.17	300.0

figures show a general agreement between the two methods both in flow structures, such as the shock positions and angles as well as the resulting temperature distribution. Also the composition of the fluid as displayed by the O mass fraction, exhibits a good agreement.

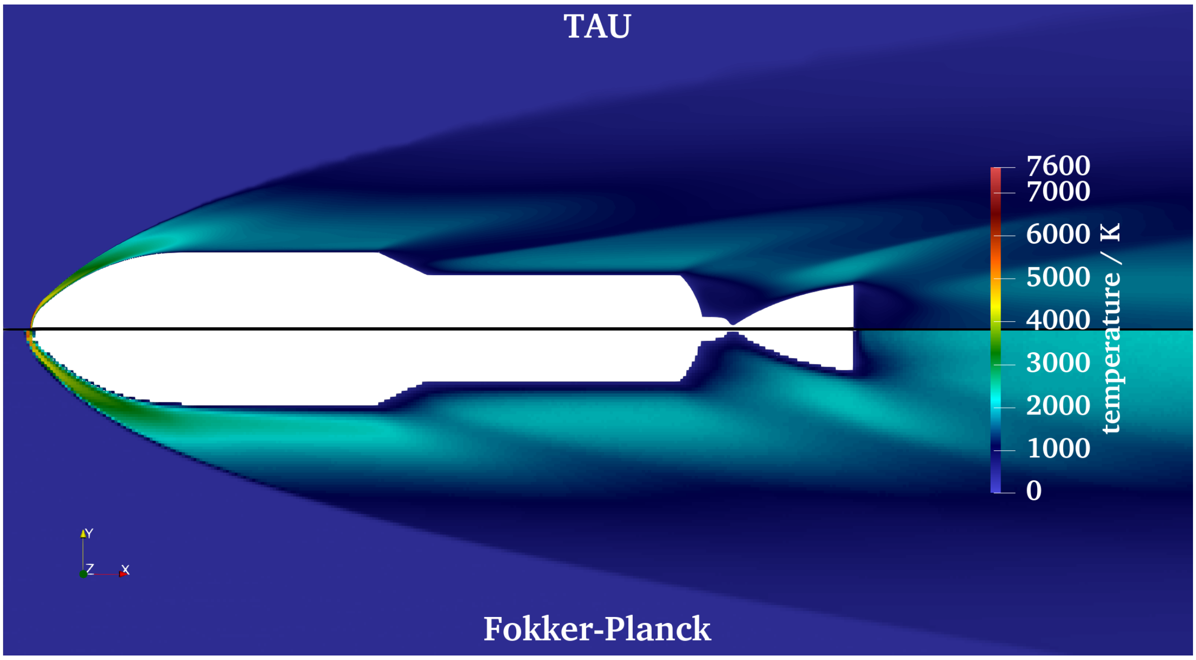

Fig 4. RFZ-ST2 upper stage with $O_2 + O \longrightarrow 3\,O$ dissociation reaction. Temperature field.

There are visible differences between the two methods, for example in the region between the base and the nozzle and behind the nozzle or close to the wall at the lower diameter section. These are in agreement with previously observed discrepancies, as have been observed and described in [9] and [10] and are therefore attributed to existing differences in the methods and not the chemical modelling.

6. Conclusion

This work is a step in our efforts towards verifying our Fokker-Planck implementation for large scale simulations of space transport vehicles and technologies. In this work a novel approach to model chemical reactions in the FP framework is compared to our well validate CFD code TAU. We described the methods for non-equilibrium chemical reactions based on a temperature dependent modified Arrhenius equation and the necessary parameters for matching results. Throughout this work we limit the chemical modeling to a single dissociation reaction of O_2.

We first used a 0D reactor to verify the temporal behaviour of the implementation. We identified the modelling of the reaction temperature for the Arrhenius equation and the modelling of the thermodynamics as areas where adaptation was needed. With the adapted parameters we are able to achieve a very good matching of the temporal evolution of temperatures and mass fractions in the 0D reactor.

We used a 2D cylinder in a $Ma = 15$ flow for a simple reacting flow verification case. We observed a good general agreement between the two methods with both the flow field and the mass fractions matching. We also observed a difference in shock stand off distance which we attribute to a modeling

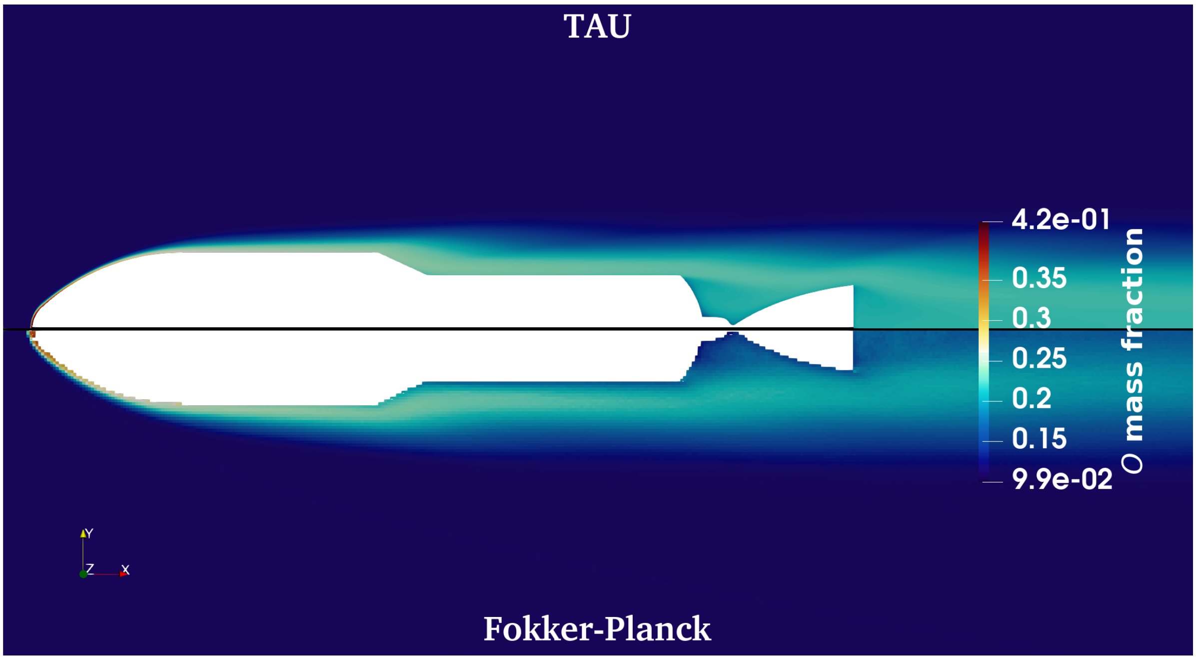

Fig 5. RFZ-ST2 upper stage with $O_2 + O \longrightarrow 3\,O$ dissociation reaction. O mass fraction field.

of the relaxation for mixtures and not the chemical reaction.

We used a 2D model of the RFZ-ST2 upper stage for a real scale space transport system verification case. We, again, observed a good general agreement between the two methods with both the flow field and the mass fractions matching. This confirms the suitability of the implemented method of non-equilibrium chemistry modelling to the large scale cases we will investigate in the future.

The presented results provide a first verification of the non-equilibrium chemical modelling in our Fokker-Planck implementation. Further steps are, however, needed including the extension to more reactions and the testing of recombination reactions. Furthermore, additional developments for improving the mixture modeling and the modeling for variable particle weights are planned.

Acknowledgements

The authors gratefully acknowledge the scientific support and HPC resources provided by the German Aerospace Center (DLR). The HPC system CARO is partially funded by ”Ministry of Science and Culture of Lower Saxony” and ”Federal Ministry for Economic Affairs and Climate Action”.

References

[1] Moritz Ertl, Tobias Ecker, Joseph Klevanski, Sven Krummen, and Etienne Dumont. Aerothermal analysis of plume interaction with deployed landing legs of the callisto vehicle. In *9th European Conference for Aeronautics and Space Sciences*, 2022.

[2] Mariasole Laureti and Sebastian Karl. Aerothermal databases and load predictions for retro propulsion-assisted launch vehicles (retalt). *CEAS Space Journal*, 2022.

[3] Ansgar Marwege, Johannes Riehmer, Josef Klevanski, Ali Gülhan, Tobias Ecker, Bodo Reimann, and Etienne Dumont. First wind tunnel data of callisto - reusable vtvl launcher first stage demonstrator. In *8th European Conference for Aeronautics and Space Sciences*, Madrid, Spain, July 2019.

[4] Ansgar Marwege, Daniel Kirchheck, and Ali Gülhan. First hot combustion subsonic retro propulsion tests in the vertical free jet facility cologne (vmk). In *HiSST: 3rd International Conference on High-Speed Vehicle Science Technology*, April 2024.

[5] Tamas Bykerk, Sebastian Karl, Moritz Ertl, Mariasole Laureti, and Tobias Ecker. Retro-propulsion in rocket systems: Recent advancements and challenges for the prediction of aerodynamic characteristics and thermal loads. *Progress in Aerospace Sciences*, 151(101044):1–32, November 2024.

[6] Christian Hepp, Martin Grabe, and Klaus Hannemann. Master equation approach for modeling diatomic gas flows with a kinetic Fokker-Planck algorithm. *Journal of Computational Physics*, 418:109638, October 2020.

[7] Klaus Hannemann, Jan Martinez Schramm, Alexander Wagner, Sebastian Karl, and Volker Hannemann. A closely coupled experimental and numerical approach for hypersonic and high enthalpy flow investigations utilising the heg shock tunnel and the dlr tau code. Technical report, DLR, 2010.

[8] Leo Basov and Martin Grabe. Modeling of polyatomic gases in the kinetic fokker-planck method by extension of the master equation approach. In *AIP Conference Proceedings*, volume 2996, page 060004. AIP Publishing, 2024.

[9] Leo Basov, Moritz Ertl, and Tamas Bykerk. Comparison of focker-planck and cfd simulations of the rfz-st2 upper stage. In *HiSST: 3rd International Conference on High-Speed Vehicle Science & Technology, 14–19 April 2024, Busan, Korea*, 2024.

[10] Moritz Ertl and Leo Basov. Comparison between the kinetic fokker-planck and tau navier-stokes simulations of hypersonic air flow around the the rfz-st2 upper stage. In *The 33rd International Symposium on Rarefied Gas Dynamics (RGD33), Göttingen*, 2024.

[11] Leo Basov, Georgii Oblapenko, and Martin Grabe. Modeling of chemical reactions in rarefied gas flows by the kinetic Fokker–Planck method. *Physics of Fluids*, 37(6):066126, June 2025.

[12] Moritz Ertl and Tamas Bykerk. A standard model for the investigation of aerodynamic and aerothermal loads on a re-usable launch vehicle - second stage geometry. In *HiSST: 3rd International Conference on High-Speed Vehicle Science & Technology, 14–19 April 2024, Busan, Korea*, Busan, Korea, April 2024.

[13] Tamas Bykerk. The rfz model - a standard model for the investigation of aerodynamic and aerothermal loads on a re-usable launch vehicle. `https://zenodo.org/communities/rfz-model`. Accessed: 2023-09-16.

[14] Leo Basov. Modeling of nozzle flow and plume impingementby a hybrid fp-dsmc method. In *HiSST: 4th International Conference onHigh-Speed Vehicle Science & Technology, 22–26 September 2025, Tours, France*, 2025.

[15] D. Schwamborn, T. Gerhold, and R. Heinrich. The dlr tau-code: recent applications in research and industry. In *ECCOMAS CFD 2006 CONFERENCE*, 2006.

[16] Yasuhiro Wada and Meng-Sing Liou. A flux splitting scheme with high-resolution and robustness for discontinuities. In *32nd Aerospace Sciences Meeting and Exhibit*, 1994.

[17] L.D. Landau and E. Teller. On the Theory of Sound Dispersion. In *Collected Papers of L.D. Landau*, pages 147–153. Elsevier.

[18] Roger C. Millikan and Donald R. White. Systematics of Vibrational Relaxation. *The Journal of Chemical Physics*, 39(12):3209–3213, 12 1963.

[19] S. J. Plimpton, S. G. Moore, A. Borner, A. K. Stagg, T. P. Koehler, J. R. Torczynski, and M. A. Gallis. Direct simulation Monte Carlo on petaflop supercomputers and beyond. *Physics of Fluids*, 31(8):086101, August 2019.

[20] Patrick Jenny, Manuel Torrilhon, and Stefan Heinz. A solution algorithm for the fluid dynamic equations based on a stochastic model for molecular motion. *Journal of Computational Physics*, 229(4):1077–1098, February 2010.

[21] Christian Hepp, Martin Grabe, and Klaus Hannemann. Master equation approach for modeling diatomic gas flows with a kinetic Fokker-Planck algorithm. *Journal of Computational Physics*, 418:109638, October 2020.

[22] Christian Hepp, Martin Grabe, and Klaus Hannemann. A kinetic Fokker–Planck approach to model hard-sphere gas mixtures. *Physics of Fluids*, 32(2):027103, February 2020.

[23] Christian Hepp, Martin Grabe, and Klaus Hannemann. A kinetic Fokker–Planck approach for modeling variable hard-sphere gas mixtures. *AIP Advances*, 10(8):085219, August 2020.

[24] M. H. Gorji, M. Torrilhon, and P. Jenny. Fokker–Planck model for computational studies of monatomic rarefied gas flows. *Journal of Fluid Mechanics*, 680:574–601, August 2011.

[25] Chul Park, John T. Howe, Richard L. Jaffe, and Graham V. Candler. Review of chemical-kinetic problems of future nasa missions. ii - mars entries. *Journal of Thermophysics and Heat Transfer*, 8(1):9–23, 1994.

[26] M. Capitelli, G. Colonna, D. Giordano, L. Marraffa, A. Casavola, P. Minelli, D. Pagano, L. D. Pietanza, F. Taccogna, and B. Warmbein. Tables of internal partition functions and thermodynamic properties of high-temperature mars-atmosphere species from 50k to 50000k. Technical Report STR 246, ESA, 2005.

[27] David G. Goodwin, Harry K. Moffat, Ingmar Schoegl, Raymond L. Speth, and Bryan W. Weber. Cantera: An object-oriented software toolkit for chemical kinetics, thermodynamics, and transport processes. `https://www.cantera.org`, 2024. Version 3.1.0.